NH_3 Converts Criegee Intermediates to Nitrogenous Organics

Xiaoying Li[1,2], Long Jia[1,2], Yongfu Xu[2,3]

[1]State Key Laboratory of Atmospheric Environment and Extreme Meteorology, Institute of Atmospheric Physics, Chinese Academy of Sciences, Beijing, 100029, China
[2]College of Earth and Planetary Sciences, University of Chinese Academy of Sciences, Beijing, 100049, China
[3]State Key Laboratory of Atmospheric Boundary Layer Physics and Atmospheric Chemistry, Institute of Atmospheric Physics, Chinese Academy of Sciences, Beijing, 100029, China

Correspondence to: Long Jia (jialong@mail.iap.ac.cn)

Abstract graphic

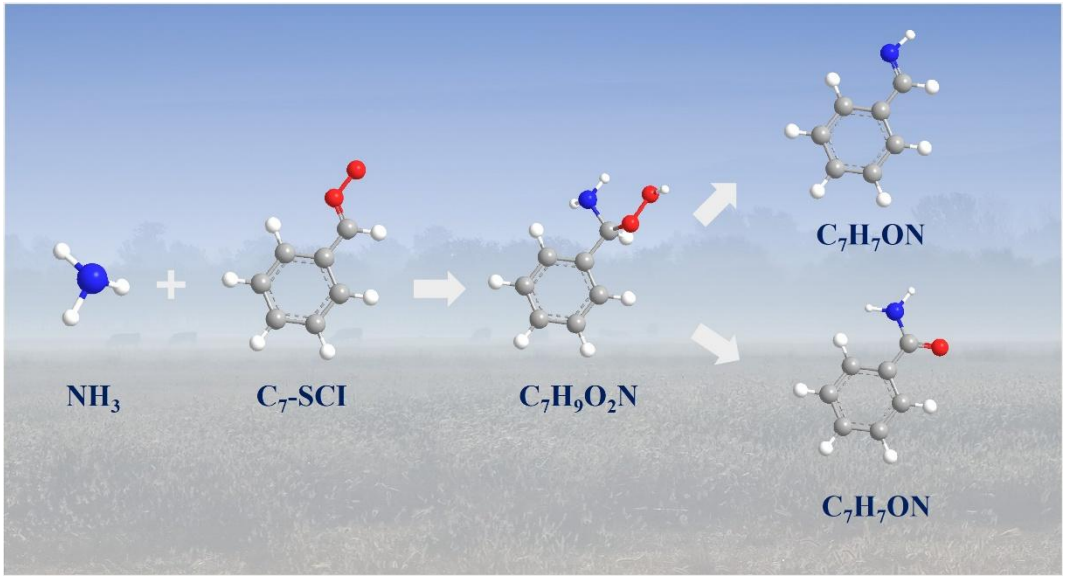

Abstract. Ammonia (NH_3), the dominant alkaline gas in the atmosphere, plays a critical role in urban air quality, but its molecular-level interactions with organics remain poorly understood. Here, we uncover a hidden chemical pathway: NH_3 efficiently scavenges stable Criegee intermediates (SCI) - critical zwitterions in organic aerosol formation. Using high-resolution Orbitrap mass spectrometry, we capture the first real-time evidence of NH_3 reacting with styrene-derived C_7-SCI to form a hazardous peroxide amine ($C_7H_9O_2N$) while suppressing traditional SCI-driven aerosol components like benzoic acid and oligomers. Due to unstable bond of peroxide in the molecule, $C_7H_9O_2N$ can further decompose into more stable compounds (imine C_7H_7N and amide C_7H_7ON). This study discovered a critical reaction pathway for the formation of organic amines through the reaction of NH_3 and SCI, which not only bridges a critical gap in understanding NH_3's role in aerosol chemistry but also exposes a previously overlooked health risk from nitrogen-enriched particulate matter.

1 Introduction

Secondary organic aerosols (SOA) are critical components of atmospheric fine particles, typically formed by the oxidation of volatile organic compounds (VOCs) (Ehn et al., 2014; Hallquist et al., 2009). SOA can significantly impact air quality and climate by scattering and absorbing sunlight, and affect human health due to their ability to reach deep into lungs(Calvin et al., 2023; Kroll and Seinfeld, 2008). Among SOA components, nitrogen-containing organic compounds (NOCs) are of particular importance due to their potential toxicity and role in light absorption(Laskin et al., 2025; Li et al., 2025; Yu et al., 2024c).

Ammonia (NH_3) is the most abundant alkaline gas in the atmosphere and plays a significant role in aerosol chemistry(Behera et al., 2013; Krupa, 2003). Global NH_3 emissions have been increasing in recent years, largely due to agricultural and industrial activities, yet models have not accounted for its potential to influence SOA(Fu et al., 2017; Meng et al., 2020; Zhang et al., 2023). NH_3 is known to enhance SOA yields by acid-base reactions(Du et al., 2023; Li et al., 2018; Lv et al., 2022; Zhang et al., 2023), and previous studies have focused on NOCs formation via reactions between NH_3 and carbonyl compounds(Laskin et al., 2014; Liu et al., 2021, 2023). Quantum calculations suggest that NH_3 may influence the SOA formation from styrene through reactions with stable Criegee intermediates (SCIs) (Ma et al., 2018; Banu et al., 2018), and NH_3 and H_2O have a synergic effect on the reaction of C_1-Criegee intermediate (Chao et al., 2019a,b). The reaction rate between NH_3 and C_1-Criegee intermediate (CH_2OO) has been determined by theoretical calculations (Jørgensen and Gross, 2009; Misiewicz et al., 2018) and experiments (Liu et al., 2018; Chao et al., 2019; Chhantyal-Pun et al., 2019). Our recent study has shown new laboratory evidence that NH_3 can also react with isoprene-derived SCIs to form NOCs, thereby changing the chemical characteristics of SOA(Li et al., 2024).

Styrene is an important anthropogenic VOC emitted from industrial processes and vehicle exhaust(Cui et al., 2022; Okada et al., 2012), and is a key precursor to urban SOA(Sun et al., 2016; Wu and Xie, 2018). The typical atmospheric concentration of styrene varies between urban and industrial areas from 0.06 to 45 ppb (Okada et al., 2012; Cho et al., 2014; Sun et al., 2016; Sheng et al., 2018). Under typical atmospheric conditions, about 30% of styrene may be consumed by O_3, thus ozone oxidation is an important sink for styrene, especially in areas with high O_3 pollution. Styrene ozonolysis can generate two types of SCI, namely C_1-SCI (CH_2OO) and C_7-SCI (C_7H_6OO) (Tuazon et al., 1993). Our studies have shown that C_1 and C_7 -SCIs play a key role in SOA formation through oligomerization(Tajuelo et al., 2019; Yu et al., 2022). Styrene is a unique aromatic with both aromatics and alkenes properties due to the containing of an aromatic ring and a highly reactive double bond in the molecule. Our recent study revealed that NH_3 can greatly suppress biogenic SOA formation from isoprene by the reaction with SCIs, which can change pathways from oligomerization to the formation of small molecular nitrogenous products(Li et al., 2024). However, it is still unknown whether this mechanism is applicable to all alkenes, especially anthropogenic sources of aromatic hydrocarbons such as styrene.

In this study, we investigate the reactions between NH_3 and styrene-derived products and their role in SOA formation. Combining chamber experiments, molecular-level measurements through Orbitrap-MS, and iodometry kinetic control experiments, we confirm that NH_3 can react with Criegee intermediates to form a peroxide amine ($C_7H_9O_2N$) and identify its

decomposition products (C_7H_7N and C_7H_7ON). Our results reveal a common pathway in both biogenic and anthropogenic alkene VOCs, where NH_3 can change Criegee intermediates chemistry toward nitrogen-containing products with reactive peroxide, which may enhance aerosol toxicity. This study bridges a critical gap in understanding the role of NH_3 in urban aerosol chemistry and highlights the need to refine SOA predictions in NH_3-polluted regions.

2 Materials and methods

Experiments and Measurements: The chamber experiments were conducted in Fluorinated Ethylene Propylene (FEP, 200A, DuPont) reactors under dark conditions, with background air supplied by purified zero air. Styrene was injected into the reactor with zero air using a glass microsyringe, O_3 was produced by an ozone generator with pure O_2, and NH_3 was directly injected into the reactor. The reactants and their concentration ranges used in the experiment are styrene (0.3~3 ppm), O_3 (1~10 ppm), and NH_3 (0~10 ppm), respectively. Because ozonolysis of styrene can form OH radicals, n-Hexane was used as an OH radical scavenger (>100ppm with a removal efficiency >90%). Detailed experimental conditions are provided in Table S1.

To collect particles and determine the SOA yields, experiments 1-5 were conducted in a 1.2 m^3 chamber. During these experiments, styrene was measured online using a proton transfer reaction-mass spectrometer (PTR-MS P1000-L-AI, Anhui Province Key Laboratory of Medical Physics and Technology) with a time resolution of 20 s in the gas phase. O_3 was measured every 0.5 hours lasting for 5 minutes with an O_3 analyzer (Model 49C, Thermo Scientific) with a time resolution of 10 s in the gas phase. The particle concentrations and size distributions were determined by a scanning mobility particle sizer (SMPS, Model 3936, DMA-3080, CPC-3776, TSI) with a time resolution of 5 minutes. The online measurements covered the entire experimental process (4~5h). Particles were collected on a 25 mm polytetrafluoroethylene (PTFE) membrane with a pore size of 0.45 μm at the 4^{th} hour, and the sample flow rate was 6 L/min and lasted for 40 min. The collected particles were extracted with methanol for composition analysis in the particle phase, which were injected by a high-performance liquid chromatography (HPLC, Thermo Scientific), ionized by a heated electrospray ionization source (ESI), and then the molecular composition was measured by a high-resolution Orbitrap mass spectrometer (Orbitrap MS, Q-Exactive, Thermo Scientific) with a resolution R= 70,000 at m/z 200. To determine the kinetics and mechanism of the reaction between C_7-SCI and NH_3, experiments 6-10 were performed with higher concentrations in a 150 L chamber. During these experiments, the products were online ionized by a gas aerosol in-situ ionization source (GAIS), and then measured by Orbitrap MS in the gas phase. The time resolution of GAIS-Orbitrap MS measurement is about 0.5 s, and all the experiments lasted about 1 h.

To detect peroxides in the sample, experiment 11 was conducted in the 1.2 m^3 chamber. The collected sample was immediately extracted by 400μL acetonitrile (ACN) before being injected into HPLC-HRMS. Using ACN as extraction solvent to minimize other unwanted decomposition processes such as hydrolysis. Half of the liquid (180 μL) from the combined extract mixed with 10 μL acetic acid (600 mM in ACN) in a vial, followed by the addition of 10 μL KI (99.5%, Sigma-Aldrich) (400 mM in H_2O) to trigger the iodometry reaction; another 180 μL aliquot was treated in a same way by adding 10 μL acetic acid

(600 mM in ACN) and 10 μL H_2O, instead of KI. These two SOA samples are designated as KI-treated and non-treated respectively, which were injected into HPLC-HRMS (Li et al., 2025).

Data Analysis and Toxicity calculation: Raw spectra were processed using Xcalibur (v4.1.31.9, Thermo Scientific). Tandem MS (MS^2) was used to determine molecular structures, and Mass Frontier (v7.0.5.9, Thermo Scientific) can simulate potential product ions for molecule with known structure, which were then compared to the MS^2 spectra of molecular ion species to confirm the final structures of the molecules. Gas-phase reactions were simulated using the Master Chemical Mechanism (MCM v3.3.1, website: https://mcm.york.ac.uk/MCM). To evaluate the influence of NH_3-SCI reactions, we added four reactions to the MCM mechanism, including those between NH_3 and C_1-/C_7-SCIs (CH_2OO/PHCHOO) and the subsequent decomposition of $C_7H_9O_2N$ into C_7H_7N and C_7H_7ON. (Bloss et al., 2005; Jenkin et al., 2003; Jia et al., 2023; Jia and Xu, 2021). The OECD QSAR Toolbox (Version 4.7, http://qsartoolbox.org) is used for the calculation of molecular toxicity, and additional details are presented in the supplementary material.

3 Results and discussion

3.1 NH_3 suppresses SOA formation from styrene

As NH_3 concentrations increased, SOA mass yields decreased significantly from (4.9±0.3) % (0 ppm NH_3) to (1.0±0.1) % (0.8 ppm NH_3), showing an obvious inhibitory effect (Fig.1a). The observed yields with 0 ppm NH_3 are within the range of those previously reported for styrene ozonolysis under no NH_3 conditions (2.7%~6.5%) (Bracco et al., 2019; Díaz-de-Mera et al., 2017; Yu et al., 2022, 2024b), which demonstrates the rationality of our experiments. A strong negative correlation was observed between NH_3 levels and SOA yields (R^2=0.98), confirming significant suppression of SOA by the presence of NH_3. In the styrene-O_3 reaction system, SOA is primarily derived from SCI-related products. As the concentration of NH_3 increases, the SOA concentration decreases linearly. This indicates that the observed reduction of SOA is attributed to the competitive consumption of SCI by NH_3.

MS analysis reveals that NH_3 suppresses SOA formation by affecting oligomerization pathways of styrene-derived SCIs. As shown in Fig.1b, the most significant peaks $C_6H_{14}O_9Na^+$ (m/z=253.052), $C_5H_{12}O_7Na^+$ (m/z=207.047) and $C_{13}H_{20}O_{11}Na^+$ (m/z=375.089) exhibit regular mass differences corresponding to C_1-SCI (CH_2OO, Δ m/z = 46.005) and C_7-SCI (C_7H_6OO, Δ m/z=122.036), consistent with our previous works that the oligomerization of SCIs is the main mechanism for SOA formation from styrene(Yu et al., 2022). These oligomers are significantly reduced by 51% with increasing NH_3 concentrations, which strongly supports the result that NH_3 can inhibit the formation of oligomers from SCIs.

Meanwhile, benzoic acid ($C_7H_5O_2^-$, m/z=121.028), as the dominant compound in styrene-ozonolysis system, is significantly suppressed by 51% with increasing NH_3 concentration (Fig.1c), which is consistent with the trend of SOA yield inhibition (50%). Since benzoic acid is mainly formed from the reaction of C_7-SCI with H_2O (Na et al., 2006; Banu et al., 2018), the presence of NH_3 apparently competes with H_2O for SCIs and inhibits the formation of benzoic acid (Fig.1d). In

addition, to maximize the potential of NH_3 and H_2O to compete for C_7-SCI under extreme conditions, we further conducted two experiments with low NH_3/normal humidity vs. high NH_3/extremely low humidity. The strong suppression on the formation of benzoic acid can be most clearly demonstrated when the concentration of NH_3 is much higher than that of H_2O. Experimental observation show that benzoic acid was suppressed by over 90% under high NH_3 concentration (10 ppm) and low relative humidity (2%) conditions (Fig.1d). The simulation results from MCM show that high concentration NH_3 (10 ppm) can suppress benzoic acid formation over 70% at 2%RH, and 50% inhibition at 17%RH. This inhibition intensifies to 80% when comparing high-NH_3/2%RH to low-NH_3/17%RH conditions. The consistency between the results from ESI, GAIS and MCM simulation confirms the role of NH_3 in competitively reacting with C_7-SCI.

Since C_7-SCI-derived products (oligomers and benzoic acid) were greatly suppressed with the presence of NH_3, where did C_7-SCIs go? Our previous study on the isoprene-ozonolysis system found that NH_3 can react with SCIs to produce amines, thereby inhibiting the original oligomerization pathway of SCIs and reducing SOA yields(Li et al., 2024). This is consistent with the phenomenon observed in this study and may be due to the same mechanisms, indicating that the reaction between NH_3 and SCIs may be common in alkenes.

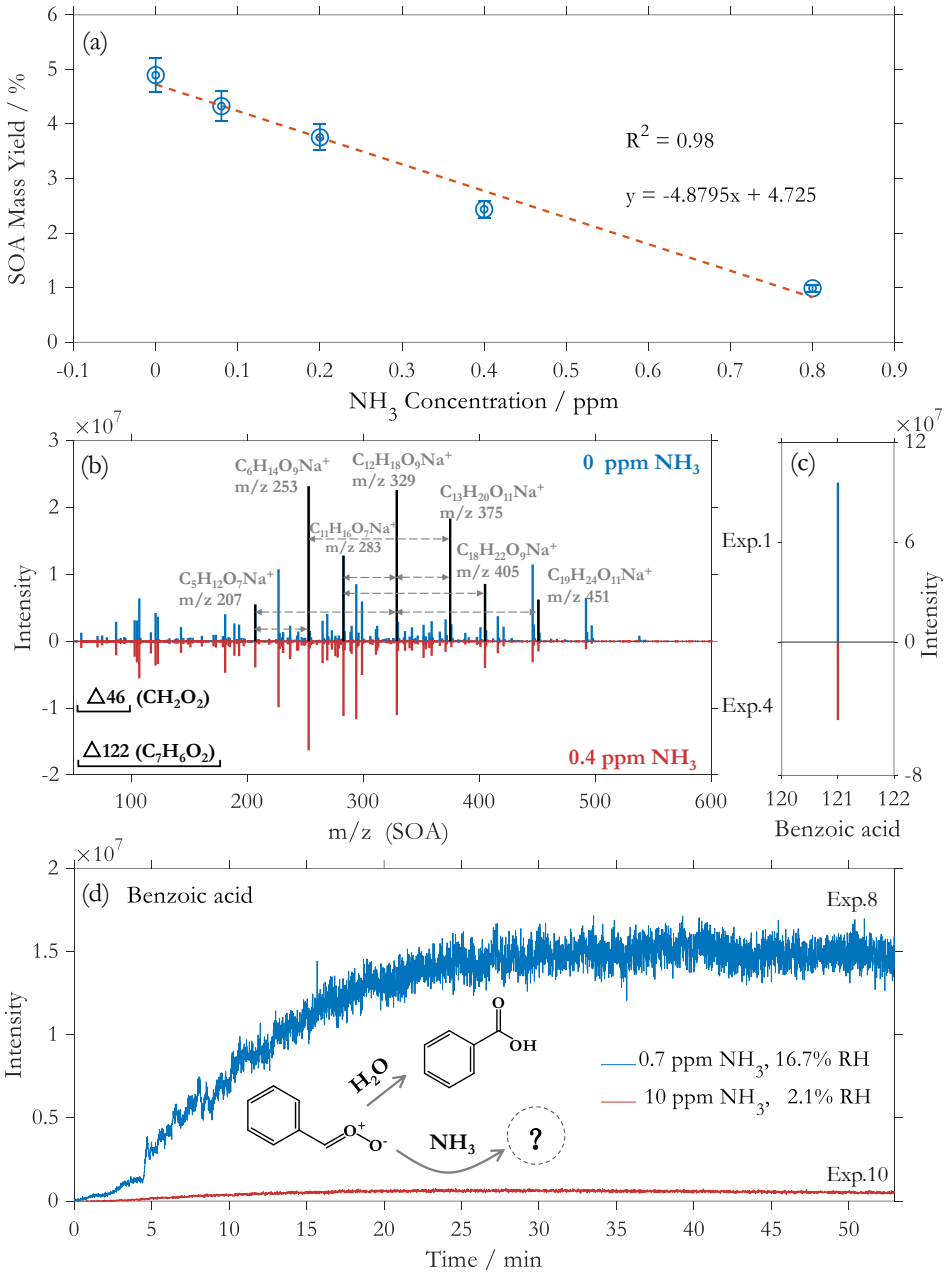

Figure 1: SOA mass yields from styrene ozonolysis under different NH_3 concentrations (a); Positive mode mass spectra of SOA from styrene ozonolysis systems with 0 ppm (blue) and 0.4 ppm NH_3 (red) (b), several top ion peaks assigned to SCI-derived oligomer are marked in black; The mass spectra of benzoic acid from styrene ozonolysis systems with 0 ppm (blue) and 0.4 ppm NH_3 (red) (c);
135 **Online observation of benzoic acid in the experiments with low concentration NH_3 with normal humidity (Ex.8, blue) and high concentration NH_3 with low humidity (Ex.10, red) (d).**

3.2 Validation of the reaction pathway between NH_3 and SCI

Referring to the reaction mechanism between C_1-SCI and NH_3 (Jørgensen and Gross, 2009; Misiewicz et al., 2018; Liu et al., 2018; Chao et al., 2019a, b; Chhantyal-Pun et al., 2019), and the reaction mechanism between C_4-SCI and NH_3 from isoprene (Li et al., 2024), C_7-SCI should react with NH_3 to produce a molecule $C_7H_9O_2N$. Online GAIS-Orbitrap MS measurements identified a nitrogen-containing product at m/z 140.071 with the molecular formula $C_7H_{10}O_2N^+$ (Fig.2a), which is in good agreement with the predicted product $C_7H_9O_2N$. However, it should be noted that the ammonium adduct ion of benzoic acid is also 140, and its molecular formula is the same as $C_7H_{10}O_2N^+$ ($C_7H_6O_2$+NH_4^+, m/z 140.071). We worried that this might affect the determination of $C_7H_{10}O_2N^+$. Therefore, to rule out the potential interference introduced by benzoic acid-ammonium adducts, we first compared the MS^2 spectra of m/z 140.071 ($C_7H_{10}O_2N^+$) and benzoic acid. Since ammonium ions are easily separated, the MS^2 of the ammonium adduct ion of benzoic acid may be mainly from m/z 123.044 ($C_7H_7O_2^+$). Results show that the MS^2 $C_7H_{10}O_2N^+$ (m/z 140.071) is different to the MS^2 $C_7H_7O_2^+$ (m/z 123.044) (Fig.2b). Different MS^2 spectra confirm that the molecule $C_7H_{10}O_2N^+$ is a unique new amine species, rather than an ammonium adduct derived from benzoic acid. We also conducted online observations by introducing NH_3 into pure benzoic acid vapor and found that no signal at m/z 140.071was detected, thus excluding the possibility of adducts. These prove that ($C_7H_{10}O_2N^+$) is not an adduct ion of benzoic acid and NH_4^+, but a newly generated species.

Based on our previous study on the reaction mechanism between NH_3 and SCI from isoprene, the molecule $C_7H_{10}O_2N^+$ (m/z 140.071) should contain a peroxide bond. To determine the presence of peroxide bond in the molecule of $C_7H_{10}O_2N^+$, we further conducted iodometry kinetic experiments based on the selective reaction of I^- ions with peroxide bonds. The chromatographic results of iodometry kinetic experiments showed that the peak of $C_7H_{10}O_2N^+$ appeared at 21.07 min. While in the control sample with added KI, its peak intensity at 21.07 min was suppressed by almost 100% (Fig.2a). This verifies the presence of a peroxide bond in $C_7H_{10}O_2N^+$, and meanwhile also confirms the molecular structure of the product from the reaction between C_7-SCI and NH_3.

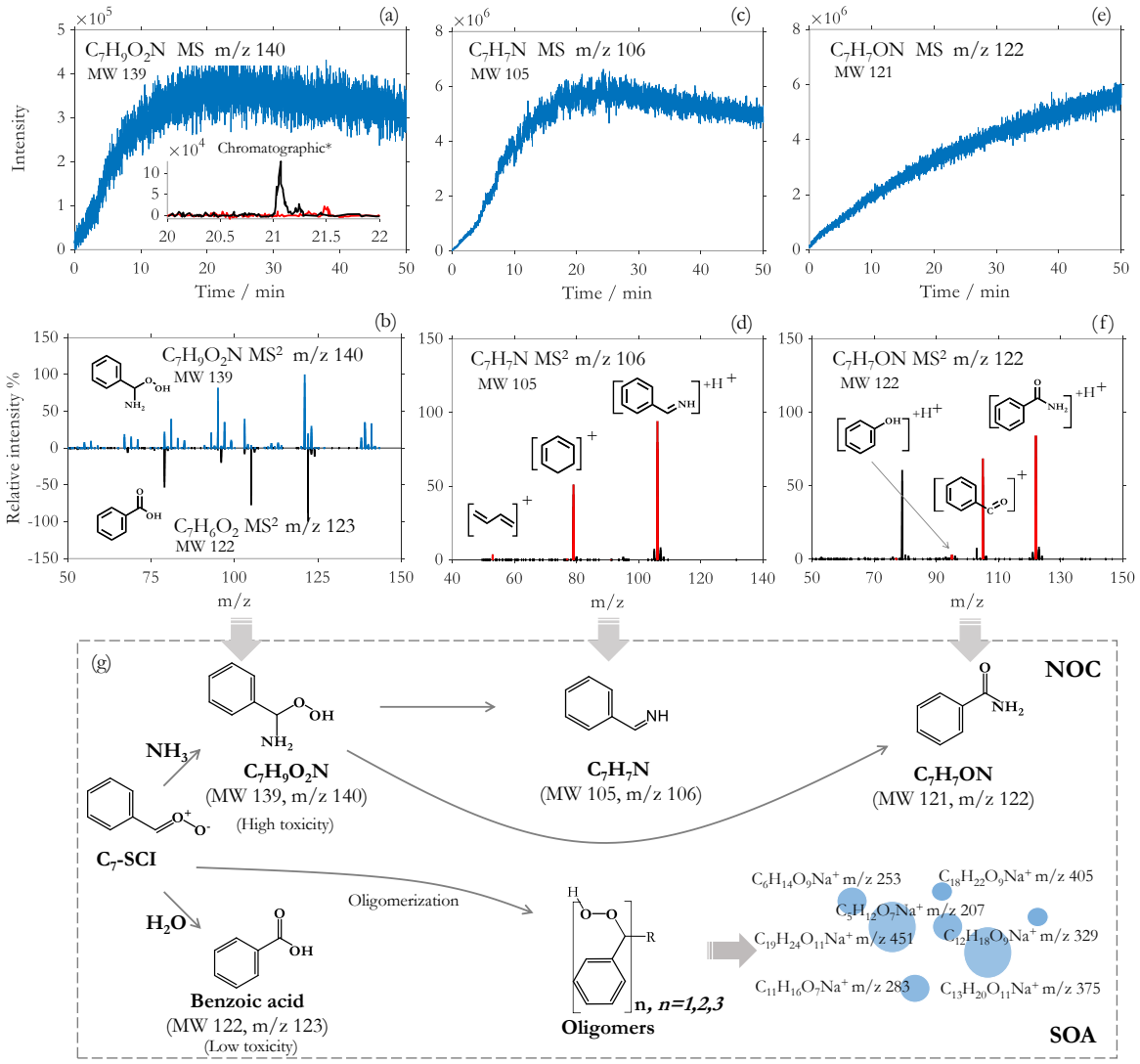

Figure 2: Time series of online observation (a) and the chromatograms of molecule $C_7H_9O_2N$ (MW 139, m/z 140.071) are shown as an inset with the initial non-KI-treated sample (black) and KI-treated sample (red). MS^2 spectra of $C_7H_9O_2N$ (MW 139, m/z 140.071, blue) and $C_7H_6O_2$ (MW 122, m/z 123.044, black) in positive modes (b). Time series of online observation of C_7H_7N and C_7H_7ON (c, e). The comparison of the ion peaks in the MS^2 spectra of $C_7H_8N^+$ and $C_7H_8ON^+$ (black bars) with the major simulated product ions of C_7H_7N and C_7H_7ON (red bars) (d, f). The mechanism of NH_3 effects on SOA from styrene ozonolysis in this study (g).

3.3 Fate of the products of NH_3 and SCI

Due to the high reactivity of peroxide bonds, the peroxide amine $C_7H_9O_2N$ is expected to be highly unstable and easily decomposed by removing one H_2O_2 or H_2O (Smith and March, 2020), and may further decompose into imines and amides based on theoretical calculation (Banu et al., 2018; Ma et al., 2018). Online MS measurements detected an imine $C_7H_8N^+$ (m/z=106.066) and an amide $C_7H_8ON^+$ (m/z=122.060) as the dominant products (Fig.2 c, e). We compared the MS^2 spectra of $C_7H_8N^+$ and $C_7H_8ON^+$ with the simulated fragments of C_7H_7N with imine structure and of C_7H_7ON with amide structure from Mass Frontier, respectively. Results show that the MS^2 spectra of $C_7H_8N^+$ and $C_7H_8ON^+$ matched well with the simulation results by Mass Frontier (Fig.2 d, f). These results demonstrate that the unstable $C_7H_9O_2N$ further decomposes into C_7H_7N and C_7H_7ON. Previous theoretical study calculated that the reaction between NH_3 and C_7-SCI may produce the products C_7H_7N and C_7H_7ON (Banu et al., 2018; Ma et al., 2018), which further supports our findings.

Accurate quantification of $C_7H_9O_2N$ and its degradation products typically requires the use of standard gases to establish a calibration coefficient between mass spectrometry signal abundance and actual concentration. However, due to the current unavailability of standard materials for $C_7H_9O_2N$ and its products, direct quantification is challenging. Nevertheless, a previous study (Ma et al., 2018) estimated the rate constant for the reaction of C_7-SCI with NH_3 forming $C_7H_9O_2N$ (1.65×10^{-15} cm^3 $molecule^{-1}$ s^{-1}) via quantum chemical calculations. Based on this rate constant, we added the corresponding reaction into the MCM mechanism. Under Exp.10 experimental conditions, the simulated maximum concentration of $C_7H_9O_2N$ after 50 minutes of reaction was 28 ppb. Since the decomposition of $C_7H_9O_2N$ was not considered in the simulation, this concentration actually represents the total concentration of $C_7H_9O_2N$ and its two decomposition products. To further distinguish the specific concentrations of $C_7H_9O_2N$ and its two decomposition products, it needs to determine their decomposition rate constants. Fortunately, using online GAIS-Orbitrap MS monitoring data on abundance-time evolution, we can obtain the relative proportions among the three species: $C_7H_9O_2N$ (m/z 140): C_7H_7N (m/z 106): C_7H_7ON (m/z 122). Based on this ratio, we introduced two decomposition reactions into the MCM mechanism and adjusted their rate constants so that the simulated concentration ratios matched the experimentally observed values. The corresponding concentrations of $C_7H_9O_2N$ (m/z 140), C_7H_7N (m/z 106) and C_7H_7ON (m/z 122) at the 50^{th} minute were determined to be 23.8 ppb, 1.6 ppb and 2.7 ppb in Exp. 10, with a deviation of ±17%. This allowed us to derive the two decomposition rate constants as $(3.0\pm0.4)\times10^{-5}$ s^{-1} and $(5.1\pm0.6)\times10^{-5}$ s^{-1}. To date, only Banu et al. (2018) have reported theoretical values for the two decomposition rate constants of $C_7H_9O_2N$, which are 7.02×10^{-16} s^{-1} and 1.22×10^{-13} s^{-1}, respectively. It shows that the experimentally derived decomposition rate constants are approximately eight orders of magnitude higher than the theoretical values, indicating that $C_7H_9O_2N$ is a highly unstable compound. Then, the maximum yields of $C_7H_9O_2N$, C_7H_7N and C_7H_7ON can be determined to be 8.1%, 3.0%, and 5.1% in styrene-O_3 system under conditions of Exp.10, respectively.

To quantify the expected atmospheric lifetime of $C_7H_9O_2N$, we have considered 3 primary removal pathways: (1) Reaction with OH radicals, the reaction rate constant between $C_7H_9O_2N$ and OH was estimated to be 4.77×10^{-11} cm^3 $molecule^{-1}$ s^{-1} using a tool of AOPWIN (Atmospheric Oxidation Program for Microsoft Windows) in EPI (Estimation Program Interface).

Using an average OH radical concentration of 1.0×10^6 molecules cm^{-3}, the atmospheric lifetime of τ_{OH} = 5.8 hours; (2) Photolysis: Based on the general photolysis rates of peroxides 1.3×10^{-6} s^{-1} (Roehl et al., 2007), the photolytic lifetime τ_{hv} = 214 hours; (3) Thermal decomposition: Based on our results, the decomposition rate of $C_7H_9O_2N$ is 8.1×10^{-5} s^{-1}, and its self-decomposition lifetime τ_{decomp}= 3.4 hours. The total atmospheric lifetime was calculated to be 2.1 hours based on $1/\tau=1/\tau_{OH}+1/\tau_{hv}+1/\tau_{decom}$. This suggests that $C_7H_9O_2N$ predominantly exists in the atmosphere as its more stable transformation products, namely the imine C_7H_7N and the amide C_7H_7ON.

Combining multiple experimental evidence, we propose the following reaction mechanism between NH_3 and styrene-derived products and their role in SOA formation (Fig.2g). Styrene reacts with O_3 to form C_7-SCI, which then generates benzoic acid and forms SOA through oligomerization (Yu et al., 2022; Yu et al., 2025). However, the addition of NH_3 leads to a competitive reaction between both NH_3 and H_2O with C_7-SCI, forming an unstable peroxide amine $C_7H_9O_2N$, which rapidly further produces more stable imine C_7H_7N and amide C_7H_7ON. Furthermore, due to the presence of peroxide bonds and nitrogen, toxicity calculations show that the toxicity of $C_7H_9O_2N$, C_7H_7N, and C_7H_7ON (High, class III) is significantly higher than that of benzoic acid (Low, class I) based on Cramer classification(Cramer et al., 1976).

The reaction pathway between NH_3 and SCI identified in both isoprene and styrene systems indicates a general mechanism by which NH_3 affects SOA molecular composition across in different olefin VOCs, highlighting the widespread impact of NH_3 on aerosol chemistry, independent of the type of olefins. NH_3 entering aerosols through reaction results in the generation of NOCs (e.g., amines, imines), which changes aerosol composition and potentially enhances light absorption and toxicity.(Updyke et al., 2012) NH_3 reduces SOA yields but increases NOC diversity. In recent years, NH_3 emissions have increased globally, driven by agricultural and industrial activities(Fu et al., 2017; Kuttippurath et al., 2020; Liu et al., 2018; Meng et al., 2020). Our study suggests that increasing NH_3 levels may suppress SOA from isoprene and styrene, and affect regional aerosol budgets. Further research is needed to determine whether it has an impact on other olefins. Current models ignore the role of NH_3 in SOA chemistry, and may overestimate the formation of SOA in NH_3-rich environments. Integrating the novel NOC formation pathway from NH_3 and SCI into the current model framework is crucial for improving climate and health predictions of aerosols.

Acknowledgments

This research has been supported by the National Natural Science Foundation of China (42461160326, 42477492, 42175125), the Strategic Priority Research Program (B) of the Chinese Academy of Sciences (XDB0760200).

Code/Data availability

The data that support the results can be found in the appendix of the supplementary material.

Author contribution

XL conducted experiments, data analysis, and drew graphs. LJ designs research, analyses data, and writes. YX designs, provides ideas, and modifies papers. All the authors participated in writing the paper.

Competing interests

The contact author has declared that none of the authors has any competing interests.

References

Banu, T., Sen, K., and Das, A. K.: Atmospheric Fate of Criegee Intermediate Formed During Ozonolysis of Styrene in the Presence of H_2O and NH_3: The Crucial Role of Stereochemistry, J. Phys. Chem. A, 122, 8377–8389, https://doi.org/10.1021/acs.jpca.8b06835, 2018.

Behera, S. N., Sharma, M., Aneja, V. P., and Balasubramanian, R.: Ammonia in the atmosphere: a review on emission sources, atmospheric chemistry and deposition on terrestrial bodies, Environ Sci Pollut Res, 20, 8092–8131, https://doi.org/10.1007/s11356-013-2051-9, 2013.

Bloss, C., Wagner, V., Jenkin, M. E., Volkamer, R., Bloss, W. J., Lee, J. D., Heard, D. E., Wirtz, K., Martin-Reviejo, M., Rea, G., Wenger, J. C., and Pilling, M. J.: Development of a detailed chemical mechanism (MCMv3.1) for the atmospheric oxidation of aromatic hydrocarbons, Atmos. Chem. Phys., 2005.

Bracco, L. L. B., Tucceri, M. E., Escalona, A., Díaz-de-Mera, Y., Aranda, A., Rodríguez, A. M., and Rodríguez, D.: New particle formation from the reactions of ozone with indene and styrene, Phys. Chem. Chem. Phys., 21, 11214–11225, https://doi.org/10.1039/C9CP00912D, 2019.

Chao, W., Yin, C., Takahashi, K., and Lin, J. J.-M.: Effects of water vapor on the reaction of CH2OO with NH3, Phys. Chem. Chem. Phys., 21, 22589–22597, https://doi.org/10.1039/C9CP04682H, 2019a.

Chao, W., Yin, C., Takahashi, K., and Lin, J. J.-M.: Hydrogen-Bonding Mediated Reactions of Criegee Intermediates in the Gas Phase: Competition between Bimolecular and Termolecular Reactions and the Catalytic Role of Water, J. Phys. Chem. A, 123, 8336–8348, https://doi.org/10.1021/acs.jpca.9b07117, 2019b.

Chen, Y., Zhou, X., Liu, Y., Jin, Y., Dong, W., and Yang, X.: Kinetics of the simplest criegee intermediate CH2OO reacting with CF3CF=CF2, Chinese Journal of Chemical Physics, 33, 234–238, https://doi.org/10.1063/1674-0068/cjcp2002025, 2020.

Chhantyal-Pun, R., Shannon, R. J., Tew, D. P., Caravan, R. L., Duchi, M., Wong, C., Ingham, A., Feldman, C., McGillen, M. R., Khan, M. A. H., Antonov, I. O., Rotavera, B., Ramasesha, K., Osborn, D. L., Taatjes, C. A., Percival, C. J., Shallcross, D. E., and Orr-Ewing, A. J.: Experimental and computational studies of Criegee intermediate reactions with NH3 and CH3 NH2, Phys. Chem. Chem. Phys., 21, 14042–14052, https://doi.org/10.1039/C8CP06810K, 2019.

Cho, J., Roueintan, M., and Li, Z.: Kinetic and dynamic investigations of OH reaction with styrene, J. Phys. Chem. A, 118, 9460–9470, https://doi.org/10.1021/jp501380j, 2014.

Cramer, G. M., Ford, R. A., and Hall, R. L.: Estimation of toxic hazard—A decision tree approach, Food and Cosmetics Toxicology, 16, 255–276, https://doi.org/10.1016/S0015-6264(76)80522-6, 1976.

Cui, L., Wu, D., Wang, S., Xu, Q., Hu, R., and Hao, J.: Measurement report: Ambient volatile organic compound (VOC) pollution in urban Beijing: characteristics, sources, and implications for pollution control, Atmos. Chem. Phys., 22, 11931–11944, https://doi.org/10.5194/acp-22-11931-2022, 2022.

Díaz-de-Mera, Y., Aranda, A., Martínez, E., Rodríguez, A. A., Rodríguez, D., and Rodríguez, A.: Formation of secondary aerosols from the ozonolysis of styrene: Effect of SO2 and H2O, Atmos. Environ., 171, 25–31, https://doi.org/10.1016/j.atmosenv.2017.10.011, 2017.

Du, L., Xu, L., Li, K., George, C., and Ge, M.: NH_3 Weakens the Enhancing Effect of SO_2 on Biogenic Secondary Organic Aerosol Formation, Environ. Sci. Technol. Lett., 10, 145–151, https://doi.org/10.1021/acs.estlett.2c00959, 2023.

Ehn, M., Thornton, J. A., Kleist, E., Sipilä, M., Junninen, H., Pullinen, I., Springer, M., Rubach, F., Tillmann, R., Lee, B., Lopez-Hilfiker, F., Andres, S., Acir, I.-H., Rissanen, M., Jokinen, T., Schobesberger, S., Kangasluoma, J., Kontkanen, J., Nieminen, T., Kurtén, T., Nielsen, L. B., Jørgensen, S., Kjaergaard, H. G., Canagaratna, M., Maso, M. D., Berndt, T., Petäjä, T., Wahner, A., Kerminen, V.-M., Kulmala, M., Worsnop, D. R., Wildt, J., and Mentel, T. F.: A large source of low-volatility secondary organic aerosol, Nature, 506, 476–479, https://doi.org/10.1038/nature13032, 2014.

Fu, X., Wang, S., Xing, J., Zhang, X., Wang, T., and Hao, J.: Increasing Ammonia Concentrations Reduce the Effectiveness of Particle Pollution Control Achieved via SO_2 and NO_X Emissions Reduction in East China, Environ. Sci. Technol. Lett., 4, 221–227, https://doi.org/10.1021/acs.estlett.7b00143, 2017.

Hallquist, M., Wenger, J. C., Baltensperger, U., Rudich, Y., Simpson, D., Claeys, M., Dommen, J., Donahue, N. M., George, C., Goldstein, A. H., Hamilton, J. F., Herrmann, H., Hoffmann, T., Iinuma, Y., Jang, M., Jenkin, M. E., Jimenez, J. L., Kiendler-Scharr, A., Maenhaut, W., McFiggans, G., Mentel, T. F., Monod, A., Prevot, A. S. H., Seinfeld, J. H., Surratt, J. D., Szmigielski, R., and Wildt, J.: The formation, properties and impact of secondary organic aerosol: current and emerging issues, Atmos. Chem. Phys., 9, 5155–5236, https://doi.org/10.5194/acp-9-5155-2009, 2009.

IPCC, 2023: Climate Change 2023: Synthesis Report. Contribution of Working Groups I, II and III to the Sixth Assessment Report of the Intergovernmental Panel on Climate Change [Core Writing Team, H. Lee and J. Romero (eds.)]. IPCC, Geneva, Switzerland, 184 pp., doi: 10.59327/IPCC/AR6-9789291691647.

Jenkin, M. E., Saunders, S. M., Wagner, V., and Pilling, M. J.: Protocol for the development of the Master Chemical Mechanism, MCM v3 (Part B): tropospheric degradation of aromatic volatile organic compounds, Part B, 2003.

Jia, L. and Xu, Y.: A core-shell box model for simulating viscosity dependent secondary organic aerosol (CSVA) and its application, Sci. Total Environ., 789, 147954, https://doi.org/10.1016/j.scitotenv.2021.147954, 2021.

Jia, L., Xu, Y., and Duan, M.: Explosive formation of secondary organic aerosol due to aerosol-fog interactions, Sci. Total Environ., 866, 161338, https://doi.org/10.1016/j.scitotenv.2022.161338, 2023.

Jørgensen, S. and Gross, A.: Theoretical Investigation of the Reaction between Carbonyl Oxides and Ammonia, J. Phys. Chem. A, 113, 10284–10290, https://doi.org/10.1021/jp905343u, 2009.

Kroll, J. H. and Seinfeld, J. H.: Chemistry of secondary organic aerosol: Formation and evolution of low-volatility organics in the atmosphere, Atmos. Environ., 42, 3593–3624, https://doi.org/10.1016/j.atmosenv.2008.01.003, 2008.

Krupa, S. V.: Effects of atmospheric ammonia (NH3) on terrestrial vegetation: a review, Environmental Pollution, 124, 179–221, https://doi.org/10.1016/S0269-7491(02)00434-7, 2003.

Kuttippurath, J., Singh, A., Dash, S. P., Mallick, N., Clerbaux, C., Van Damme, M., Clarisse, L., Coheur, P.-F., Raj, S., Abbhishek, K., and Varikoden, H.: Record high levels of atmospheric ammonia over India: Spatial and temporal analyses, Sci. Total Environ., 740, 139986, https://doi.org/10.1016/j.scitotenv.2020.139986, 2020.

Laskin, A., West, C. P., and Hettiyadura, A. P. S.: Molecular insights into the composition, sources, and aging of atmospheric brown carbon, Chem. Soc. Rev., 54, 1583–1612, https://doi.org/10.1039/D3CS00609C, 2025.

Laskin, J., Laskin, A., Nizkorodov, S. A., Roach, P., Eckert, P., Gilles, M. K., Wang, B., Lee, H. J. (Julie), and Hu, Q.: Molecular Selectivity of Brown Carbon Chromophores, Environ. Sci. Technol., 48, 12047–12055, https://doi.org/10.1021/es503432r, 2014.

Li, K., Chen, L., White, S. J., Yu, H., Wu, X., Gao, X., Azzi, M., and Cen, K.: Smog chamber study of the role of NH3 in new particle formation from photo-oxidation of aromatic hydrocarbons, Sci. Total Environ., 619–620, 927–937, https://doi.org/10.1016/j.scitotenv.2017.11.180, 2018.

Li, K., Zheng, Z., Resch, J., Ma, J., Hansel, A., and Kalberer, M.: Molecular composition of organic peroxides in secondary organic aerosols revealed by peroxide-iodide reactivity, Environ. Sci. Technol., 59, 17126–17136, https://doi.org/10.1021/acs.est.5c03241, 2025.

Li, X., Jia, L., Xu, Y., and Pan, Y.: A novel reaction between ammonia and Criegee intermediates can form amines and suppress oligomers from isoprene, Sci. Total Environ., 956, 177389, https://doi.org/10.1016/j.scitotenv.2024.177389, 2024.

Li, Y., Fu, T.-M., Yu, J. Z., Zhang, A., Yu, X., Ye, J., Zhu, L., Shen, H., Wang, C., Yang, X., Tao, S., Chen, Q., Li, Y., Li, L., Che, H., and Heald, C. L.: Nitrogen dominates global atmospheric organic aerosol absorption, Science, 387, 989–995, https://doi.org/10.1126/science.adr4473, 2025.

Liu, M., Huang, X., Song, Y., Xu, T., Wang, S., Wu, Z., Hu, M., Zhang, L., Zhang, Q., Pan, Y., Liu, X., and Zhu, T.: Rapid SO_2 emission reductions significantly increase tropospheric ammonia concentrations over the North China Plain, Atmos. Chem. Phys., 18, 17933–17943, https://doi.org/10.5194/acp-18-17933-2018, 2018.

Liu, S., Huang, D., Wang, Y., Zhang, S., Liu, X., Wu, C., Du, W., and Wang, G.: Synergetic effects of NH3 and NOx on the production and optical absorption of secondary organic aerosol formation from toluene photooxidation, Atmos. Chem. Phys., 21, 17759–17773, https://doi.org/10.5194/acp-21-17759-2021, 2021.

Liu, X., Wang, H., Wang, F., Lv, S., Wu, C., Zhao, Y., Zhang, S., Liu, S., Xu, X., Lei, Y., and Wang, G.: Secondary Formation of Atmospheric Brown Carbon in China Haze: Implication for an Enhancing Role of Ammonia, Environ. Sci. Technol., 57, 11163–11172, https://doi.org/10.1021/acs.est.3c03948, 2023.

Liu, Y., Yin, C., Smith, M. C., Liu, S., Chen, M., Zhou, X., Xiao, C., Dai, D., Lin, J. J.-M., Takahashi, K., Dong, W., and Yang, X.: Kinetics of the reaction of the simplest Criegee intermediate with ammonia: a combination of experiment and theory, Phys. Chem. Chem. Phys., 20, 29669–29676, https://doi.org/10.1039/C8CP05920A, 2018.

Lv, S., Wang, F., Wu, C., Chen, Y., Liu, S., Zhang, S., Li, D., Du, W., Zhang, F., Wang, H., Huang, C., Fu, Q., Duan, Y., and Wang, G.: Gas-to-Aerosol Phase Partitioning of Atmospheric Water-Soluble Organic Compounds at a Rural Site in China: An Enhancing Effect of NH_3 on SOA Formation, Environ. Sci. Technol., 56, 3915–3924, https://doi.org/10.1021/acs.est.1c06855, 2022.

Ma, Q., Lin, X., Yang, C., Long, B., Gai, Y., and Zhang, W.: The influences of ammonia on aerosol formation in the ozonolysis of styrene: roles of Criegee intermediate reactions, R. Soc. open sci., 5, 172171, https://doi.org/10.1098/rsos.172171, 2018.

Meng, Z., Wu, L., Xu, X., Xu, W., Zhang, R., Jia, X., Liang, L., Miao, Y., Cheng, H., Xie, Y., He, J., and Zhong, J.: Changes in ammonia and its effects on PM2.5 chemical property in three winter seasons in Beijing, China, Sci. Total Environ., 749, 142208, https://doi.org/10.1016/j.scitotenv.2020.142208, 2020.

Misiewicz, J. P., Elliott, S. N., Moore, K. B., and Schaefer, H. F.: Re-examining ammonia addition to the Criegee intermediate: converging to chemical accuracy, Phys. Chem. Chem. Phys., 20, 7479–7491, https://doi.org/10.1039/C7CP08582F, 2018.

Na, K., Song, C., and Cockeriii, D.: Formation of secondary organic aerosol from the reaction of styrene with ozone in the presence and absence of ammonia and water, Atmos. Environ., 40, 1889–1900, https://doi.org/10.1016/j.atmosenv.2005.10.063, 2006.

Okada, Y., Nakagoshi, A., Tsurukawa, M., Matsumura, C., Eiho, J., and Nakano, T.: Environmental risk assessment and concentration trend of atmospheric volatile organic compounds in Hyogo Prefecture, Japan, Environ Sci Pollut Res, 19, 201–213, https://doi.org/10.1007/s11356-011-0550-0, 2012.

Roehl, C. M., Marka, Z., Fry, J. L., and Wennberg, P. O.: Near-UV photolysis cross sections of CH3OOH and HOCH2OOH determined via action spectroscopy, Atmos. Chem. Phys., 2007.

Sheng, J., Zhao, D., Ding, D., Li, X., Huang, M., Gao, Y., Quan, J., and Zhang, Q.: Characterizing the level, photochemical reactivity, emission, and source contribution of the volatile organic compounds based on PTR-TOF-MS during winter haze period in beijing, China, Atmospheric Research, 212, 54–63, https://doi.org/10.1016/j.atmosres.2018.05.005, 2018.

Sun, J., Wu, F., Hu, B., Tang, G., Zhang, J., and Wang, Y.: VOC characteristics, emissions and contributions to SOA formation during hazy episodes, Atmos. Environ., 141, 560–570, https://doi.org/10.1016/j.atmosenv.2016.06.060, 2016.

Smith, M. and March, J.: March's advanced organic chemistry : reactions, mechanisms, and structure, Eighth edition., John Wiley & Sons, Inc., Hoboken, New Jersey, 2020.

Sofen, E. D., Bowdalo, D., Evans, M. J., Apadula, F., Bonasoni, P., Cupeiro, M., Ellul, R., Galbally, I. E., Girgzdiene, R., Luppo, S., Mimouni, M., Nahas, A. C., Saliba, M., and Tørseth, K.: Gridded global surface ozone metrics for atmospheric chemistry model evaluation, 2016.

Sun, J., Wu, F., Hu, B., Tang, G., Zhang, J., and Wang, Y.: VOC characteristics, emissions and contributions to SOA formation during hazy episodes, Atmos. Environ., 141, 560–570, https://doi.org/10.1016/j.atmosenv.2016.06.060, 2016.

Tajuelo, M., Rodríguez, D., Baeza-Romero, M. T., Díaz-de-Mera, Y., Aranda, A., and Rodríguez, A.: Secondary organic aerosol formation from styrene photolysis and photooxidation with hydroxyl radicals, Chemosphere, 231, 276–286, https://doi.org/10.1016/j.chemosphere.2019.05.136, 2019.

Tuazon, E. C., Arey, J., Atkinson, R., and Aschmann, S. M.: Gas-phase reactions of 2-vinylpyridine and styrene with hydroxyl and NO3 radicals and ozone, Environ. Sci. Technol., 27, 1832–1841, https://doi.org/10.1021/es00046a011, 1993.

Updyke, K. M., Nguyen, T. B., and Nizkorodov, S. A.: Formation of brown carbon via reactions of ammonia with secondary organic aerosols from biogenic and anthropogenic precursors, Atmos. Environ., 63, 22–31, https://doi.org/10.1016/j.atmosenv.2012.09.012, 2012.

Wu, R. and Xie, S.: Spatial Distribution of Secondary Organic Aerosol Formation Potential in China Derived from Speciated Anthropogenic Volatile Organic Compound Emissions, Environ. Sci. Technol., 52, 8146–8156, https://doi.org/10.1021/acs.est.8b01269, 2018.

Yu, S., Jia, L., Xu, Y., and Pan, Y.: Formation of extremely low-volatility organic compounds from styrene ozonolysis: Implication for nucleation, Chemosphere, 305, 135459, https://doi.org/10.1016/j.chemosphere.2022.135459, 2022.

Yu, S., Jia, L., Xu, Y., and Pan, Y.: Molecular interaction between ammonium sulfate and secondary organic aerosol from styrene, Sci. Total Environ., 954, 176414, https://doi.org/10.1016/j.scitotenv.2024.176414, 2024a.

Yu, S., Jia, L., Xu, Y., and Pan, Y.: Oligomer formation from cross-reaction of Criegee intermediates in the styrene-isoprene-O_3 mixed system, Chemosphere, 349, 140811, https://doi.org/10.1016/j.chemosphere.2023.140811, 2024b.

Yu, S., Tong, S., Chen, M., Zhang, H., Xu, Y., Guo, Y., and Ge, M.: Characterization of key intermediates and products from the ozonolysis of styrene-like compounds, Environ. Sci. Technol., 59, 11666–11676, https://doi.org/10.1021/acs.est.5c00769, 2025.

Yu, X., Li, Q., Liao, K., Li, Y., Wang, X., Zhou, Y., Liang, Y., and Yu, J. Z.: New measurements reveal a large contribution of nitrogenous molecules to ambient organic aerosol, npj Clim Atmos Sci, 7, 72, https://doi.org/10.1038/s41612-024-00620-6, 2024c.

Zhang, Y., Cheng, M., Gao, J., and Li, J.: Review of the influencing factors of secondary organic aerosol formation and aging mechanism based on photochemical smog chamber simulation methods, J. Environ. Sci., 123, 545–559, https://doi.org/10.1016/j.jes.2022.10.033, 2023.